# Four-photon excitation of autoionizing states of Ar, Kr, and Xe between the $^2P_{3/2}$ and $^2P_{1/2}$ ionic limits

S. M. Koeckhoven, W. J. Buma, and C. A. de Lange
*Laboratory for Physical Chemistry, University of Amsterdam, Nieuwe Achtergracht 127, 1018 WS Amsterdam, The Netherlands*
(Received 23 June 1994)

In a previous paper [Phys. Rev. A **49**, 3322 (1994)] we reported on a three-photon excitation study of *odd* (in $j_c l$ coupling notation $nl'[K]_J$, in which the angular momentum of the ion core $j_c$ is coupled to the orbital momentum of the Rydberg electron $l$ to give $K$, which is then coupled to the electron spin to give $J$) $ns'[1/2]_1$, $nd'[3/2]_1$, $nd'[5/2]_3$, and $ng'[7/2]_3$ autoionizing series of atomic argon, krypton, and xenon. Here, four-photon excitation of *even* autoionizing Rydberg states of these rare gases between the $^2P_{3/2}$ and $^2P_{1/2}$ ionic limits has been investigated using multiphoton ionization and supersonic expansion techniques. In all atoms the $np'[1/2]_0$, $np'[3/2]_2$, $nf'[5/2]_2$, and $nf'[7/2]_4$ autoionizing series have been observed. Such states have never been observed before in argon, while in krypton and xenon our experimental conditions have enabled a considerably more accurate and extended investigation than previously possible. The analysis of the resonance line shapes and intensities has allowed for a detailed investigation of the four-photon ionization dynamics, in particular with respect to the role of the three-photon virtual level.

PACS number(s): 32.70.Jz, 32.80.Dz

## I. INTRODUCTION

For the investigation of autoionizing states of the rare gases between their $^2P_{3/2}$ and $^2P_{1/2}$ ionic limits, predominantly one-photon excitation from the ground state using vacuum ultraviolet (vuv) radiation has been applied [1–8]. The use of such an excitation scheme enables the observation of resonances deriving from $ns'[1/2]_1$ and $nd'[3/2]_1$ ($j_c l$ coupling notation) states. In order to investigate other autoionizing states more complicated excitation schemes are required, such as one-photon excitation from excited states instead of the ground state [9–14]. Though technically more demanding, such excitation schemes are rewarding, since apart from the fact that a variety of excited states becomes accessible, they generally also offer improved energy resolution as a result of the possibility of using narrow-band lasers.

Despite the increased spectrum of states that can be reached with the latter excitation schemes, the use of one-photon excitation inherently puts considerable constraints on the types of states that can be studied. An excellent alternative, which with the advent of high-power lasers has become increasingly attractive, is the application of nonresonant multiphoton excitation. In our previous study we have shown that three-photon excitation of autoionizing states of Ar, Kr, and Xe allows for a detailed investigation of the *odd* $ns'[1/2]_1$, $nd'[3/2]_1$, $nd'[5/2]_3$, and $ng'[7/2]_3$ Rydberg series [15]. In this study autoionizing states of Ar could be observed under multiphoton excitation conditions, while the knowledge of such states of Kr and Xe was considerably augmented.

In the present study *even* autoionizing Rydberg series of Ar, Kr, and Xe between their $^2P_{3/2}$ and $^2P_{1/2}$ ionic limits have been studied by four-photon absorption from the ground state. According to the selection rules, five series can be accessed under linearly polarized excitation conditions, viz., the $np'[1/2]_0$, $np'[3/2]_2$, $nf'[5/2]_2$, $nf'[7/2]_4$, and $nh'[9/2]_4$ series. In our excitation spectra all series can be assigned, except $nh'[9/2]_4$. Such even Rydberg states have, to our knowledge, not been observed before for Ar. For Kr and Xe, members of these autoionizing series have been observed previously [9,16–18], but the present experimental conditions have enabled a considerable extension of the number of members that can be observed. Moreover, the resonances of these states have been measured with an improved energy resolution allowing, e.g., for the observation of fully resolved $np'[1/2]_0$ and $np'[3/2]_2$ resonances, which previously could only barely be observed separately.

Apart from the use of linearly polarized light, excitation has also been performed with circularly polarized light. Under such conditions selection rules only allow for the excitation of $J=4$ Rydberg states, i.e., members of the $nf'[7/2]_4$ series. The comparison of excitation spectra obtained with linearly and circularly polarized light consequently provides a useful tool to reach a unique assignment of the two $nf'$ components, which will be shown to overlap under linearly polarized excitation conditions.

From an analysis of the resonance line shapes, the quantum defects, widths, and line-profile indices of the various resonances have been established. These parameters will be discussed and, where possible, compared to previous experimental and theoretical multichannel quantum-defect theory (MQDT) results. Finally, it will be shown that the four-photon ionization dynamics cannot be understood when it is assumed that only the four-phonon energy level determines the appearance of the excitation spectra. Our observation of the energy-dependent line-shape parameters, anomalously varying cross sections of members within one series, and differences between the four-photon excitation spectra of Ar, Kr, and Xe will be demonstrated to reveal the profound influence of near-resonance effects at the three-phonon virtual level.

 

## II. EXPERIMENT

In the present study the same experimental setup was used as in our previous three-photon excitation work [15]. Briefly, a supersonic expansion of pure rare gases, generated by a pulsed valve, is intersected at right angles by a focused laser beam. Ions generated at the intersection point are focused into the entrance of a quadrupole mass filter and detected by a CuBe multiplier.

The laser system consists of an excimer-pumped dye laser (bandwidth 0.08 $cm^{-1}$), which operated on the dyes DCM, DPS, Qui, B-PBD, TMQ, and PTP. In the experiments on Ar a frequency-doubling unit was employed, consisting of an autotracking unit equipped with a potassium dihydrogen phosphate crystal. In order to obtain pure linearly polarized excitation light ($10^5$:1) a Wollaston prism was used. With a Pockels cell the polarization of the laser light could be modified continuously while not affecting the intensity of the laser light, enabling the generation of circularly polarized light with a purity of 300:1.

Wavelength calibration in the experiments on Ar and Kr was achieved by recording, simultaneously with the multiphoton ionization spectrum, the accurately known optogalvanic spectrum of Ne [19], which was excited in a hollow-cathode lamp using the fundamental laser light. In the experiments on Xe the strong $6s'[1/2]_1$ and $5d[7/2]_3$ [20] (3+1) resonantly enhanced multiphoton ionization (REMPI) resonances were used for obtaining a wavelength calibration. These calibrations enabled the determination of the fundamental wavelength with an accuracy of 0.30 $cm^{-1}$. The excitation spectra shown in the present study were not corrected for variations in the laser output resulting from the dye gain curve.

In a four-photon nonresonance enhanced excitation experiment high laser intensities are a prerequisite to obtain a measurable signal intensity. One should consequently be cautious of power-broadening effects and Stark shifts. Additionally, our previous three-photon excitation experiments had indicated that also pressure effects might influence the shape and excitation energy of the resonances. Within the possible range of variation that could be applied to these parameters, it was found that the laser intensity was the major influencing factor. In the case of Ar and Xe this influence was observed, however, to be so small that the excitation energies and line-shape parameters derived from the spectra discussed in the present paper, which have been recorded using the lowest possible laser powers and gas pressures, correspond within the quoted error range to unperturbed excitation energies and line-shape parameters. In the case of Kr, on the other hand, a study of the influence of the laser power revealed that a substantial ac Stark effect should be taken into account (*vide infra*) in agreement with the results of a previous four-photon excitation study of autoionizing resonances in Kr [16]. The excitation energies and line-shape parameters derived from these spectra are consequently subject to larger error margins and correspond to perturbed values obtained at the lowest possible laser power density $\sim 6\times 10^9$ $W/cm^2$.

## III. RESULTS

In Fig. 1 the four-photon excitation spectrum of autoionizing resonances of Ar between the $^2P_{3/2}$ and $^2P_{1/2}$ ionic limits using linearly polarized excitation light is shown. In this excitation spectrum two series of resonances can be observed, one consisting of strong asymmetric features assigned to the members of the $np'$ series and one appearing as small narrow resonances deriving from the members of the $nf'$ series. Although the selection rules allow for the excitation of two components of the $np'$ series, viz., $np'[1/2]_0$ and $np'[3/2]_2$, the strong asymmetric features of the $np'$ series do not give any indication for the presence of two separate resonances, as shown in the high-resolution scan of the $12p'$ member presented in Fig. 2(a). Our results on Kr and Xe, to be described below, however, suggest that these strong asymmetric resonances actually contain the contributions of the overlapping members of the $np'[1/2]_0$ and $np'[3/2]_2$ series, each with comparable intensity. Similarly, we would have expected to observe the $nf'[5/2]_2$ and $nf'[7/2]_4$ components of the $nf'$ series. The proof that the small narrow resonances consist of the overlapping resonances of these two components is obtained by excitation with circularly polarized light. Under these conditions selection rules allow only for the excitation of states with $J=4$ whose intensity should increase by a factor of $\frac{35}{8}$. Indeed, it is observed that with circularly polarized excitation light the strong asymmetric resonances assigned to the $np'[1/2]_0$ and $np'[3/2]_2$ states disappear completely, while the signal intensities of the small narrow resonances change. The intensity ratios $S_{\rm lin}/S_{\rm cir}$ of these resonances are given in Table I. Here $S_{\rm lin}$ is the total signal intensity of the $nf'[5/2]_2$ and $nf'[7/2]_4$ resonances measured with linearly polarized excitation light and $S_{\rm cir}$ the signal intensity of the $nf'[7/2]_4$ component measured with circularly polarized light. From the observation that under circularly polarized excitation conditions the small narrow resonances do not disappear it can be concluded that they cannot be solely attributed to the $nf'[5/2]_2$ states. On the other hand, Table I shows

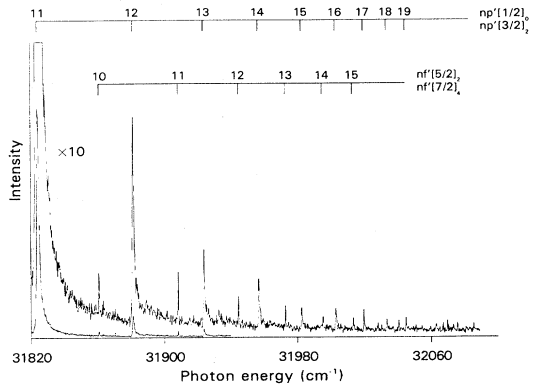


FIG. 1. Four-photon excitation spectrum of autoionizing series in Ar between the $^2P_{3/2}$ and $^2P_{1/2}$ ionic limits obtained with linearly polarized excitation light.

ratios $S_{\text{lin}}/S_{\text{cir}}$ that deviate significantly from the predicted factor $\frac{8}{35}$, which would have been expected if the resonances only derived from the $nf'[7/2]_4$ states. We therefore conclude that both the $nf'[5/2]_2$ and $nf'[7/2]_4$ components contribute significantly to the resonance signal intensities observed with linearly polarized excitation light.

A striking feature of the spectrum is that the peak intensities of the members of the $np'$ series strongly decrease as $n$ increases. This observation can only to a limited extent be explained by the dye gain curve and the laser bandwidth, which can also cause decreasing peak intensities for higher members.

The four-photon linearly polarized excitation spectrum of Kr is shown in Fig. 3. In this spectrum four series can be assigned, viz., $np'[1/2]_0$, $np'[3/2]_2$, $nf'[5/2]_2$, and $nf'[7/2]_4$. In contrast to what was observed in the case of Ar, the resonances of the $np'[1/2]_0$ and $np'[3/2]_2$ series are now well resolved, as is seen clearly in Fig. 2(b) in which a high-resolution scan of the $10p'[1/2]_0$ and $10p'[3/2]_2$ resonances is shown.

As yet the possibility that resonances deriving from the formally four-photon allowed $nh'[9/2]_4$ autoionizing Rydberg states contribute to the observed excitation spectra has not been discussed. Consideration of the quantum defects shows that for Ar, where the first observable autoionizing member would occur for $n=10$, the resonances attributed to the $nf'$ series might contain contributions of the $nh'[9/2]_4$ series. However, the excitation spectra obtained for Kr and Xe (*vide infra*) definitely exclude such a possibility. For Kr the first observable autoionizing member would be the $6h'[9/2]_4$ state. Taking into account the term values of the $6f'$ states determined in the present study and of the $6g'[7/2]_3$ state determined in our previous study [15], we find that the difference between the excitation energies of the $6h'[9/2]_4$ and $6f'$ states should be *at least* 6 $\text{cm}^{-1}$. High-quality scans of the $6f'$ excitation region of Kr reveal that no signals are present apart from the $6f'$ resonances. We therefore conclude that the $nh'[9/2]_4$ series cannot be observed under the present experimental conditions. Since a similar conclusion is obtained in our experiments on Xe (*vide infra*) we infer that also in Ar the role of the $nh'[9/2]_4$ series can be neglected.

TABLE I. In the second column the ratios $S_{\text{lin}}/S_{\text{cir}}$ (see text) of the $nf'$ resonances in Ar, Kr, and Xe are given. In the third column the ratios $S_{J=2}/S_{J=4}$, determined from the ratios $S_{\text{lin}}/S_{\text{cir}}$ using Eq. (4), are given.

| State | $S_{\text{lin}}/S_{\text{cir}}$ | $S_{J=2}/S_{J=4}$ |
|---|---|---|
| | Ar | |
| $10f'$ | 1.46 | 5.39 |
| $11f'$ | 1.32 | 4.78 |
| | Kr | |
| $5f'$ | 0.69 | 2.02 |
| $6f'$ | 1.69 | 6.39 |
| $7f'$ | 1.34 | 4.86 |
| $8f'$ | 1.26 | 4.51 |
| $9f'$ | 1.20 | 4.25 |
| | Xe | |
| $4f'$ | 0.59 | 1.58 |
| $5f'$ | 3.35 | 13.66 |
| $6f'$ | 2.79 | 11.21 |
| $7f'$ | 1.94 | 7.49 |

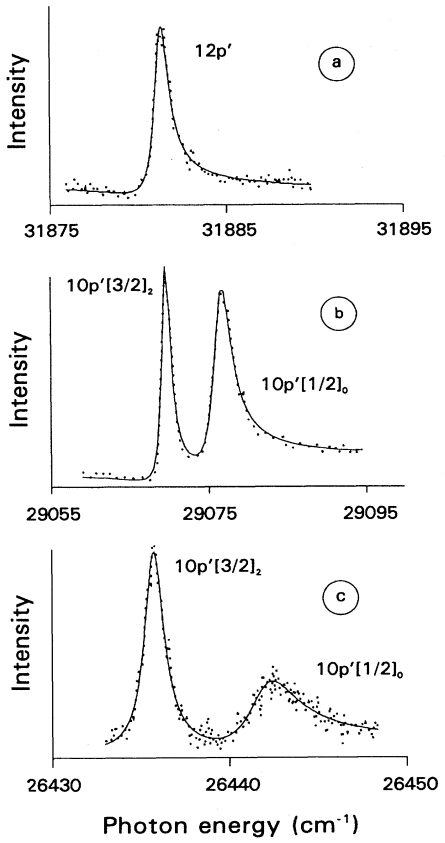


FIG. 2. High-resolution four-photon excitation spectrum using linearly polarized light of (a) the $12p'[1/2]_0$ and $12p'[3/2]_2$ autoionizing resonances of Ar, (b) the $10p'[1/2]_0$ and $10p'[3/2]_2$ autoionizing resonances of Kr, and (c) the $10p'[1/2]_0$ and $10p'[3/2]_2$ autoionizing resonances of Xe.

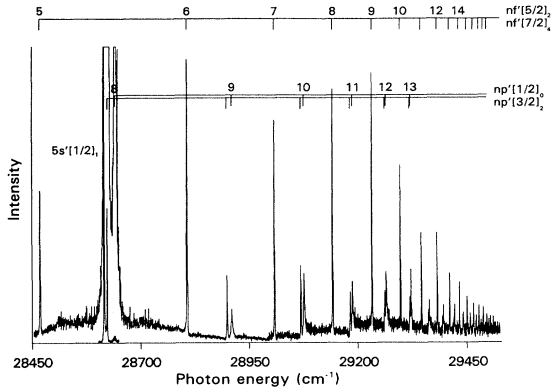


FIG. 3. Four-photon excitation spectrum of autoionizing series in Kr between the $^2P_{3/2}$ and $^2P_{1/2}$ ionic limits obtained with linearly polarized excitation light.

Members of the $nf'[5/2]_2$ and $nf'[7/2]_4$ series, which appear as strong narrow resonances, cannot be resolved using linearly polarized excitation light. For the lower members, however, a small shift of the resonances is observed when the polarization of the light is changed from linear to circular, indicating slightly different excitation energies of the $nf'[5/2]_2$ and $nf'[7/2]_4$ states. Changing the polarization also resulted in a change of the signal intensities. The ratios $S_{\text{lin}}/S_{\text{cir}}$ observed for the various members are given in Table I.

The large resonance at a one-photon energy of 28 616 $\text{cm}^{-1}$ is due to the (3+1) REMPI signal of the $5s'[1/2]_1$ state. This resonance is considerably broadened by power effects and therefore overlaps with the $8p'[1/2]_0$ and $8p'[3/2]_2$ resonances. Lowering the laser power resulted in smaller linewidths, allowing the two $8p'$ resonances to be observed, as shown in Fig. 3.

In the experiments on Kr two dyes were used to obtain the four-photon excitation spectrum between the lower two ionic limits. The two broad features in the background signal of the spectrum shown in Fig. 3 are due to these curves. Since no correction has been performed for these dye gain curves, the peak intensities of the various resonances cannot be compared directly. From the fact that the $8p'$ resonances can be observed at much lower laser powers than those necessary for the observation of the other members of these series, it can be concluded that the cross sections of the $8p'$ resonances are much larger than those of the other members.

The four-photon excitation spectrum of Xe between the $^2P_{3/2}$ and $^2P_{1/2}$ ionic limits is depicted in Fig. 4. As in the experiments on Kr and Ar, the resonances can be assigned to the $np'[1/2]_0$, $np'[3/2]_2$, $nf'[5/2]_2$, and $nf'[7/2]_4$ series. On the basis of the same arguments as presented for Kr, high-quality scans of the $6f'$ excitation region show that the $nh'[9/2]_4$ series cannot be observed in the present experiments. Similar to the excitation spectra of Kr, the resonances of the $np'[1/2]_0$ and $np'[3/2]_2$ series are well resolved up to $n=13$. In Fig. 2(c) a high-resolution scan of the $10p'[1/2]_0$ and $10p'[3/2]_2$ resonances is depicted.

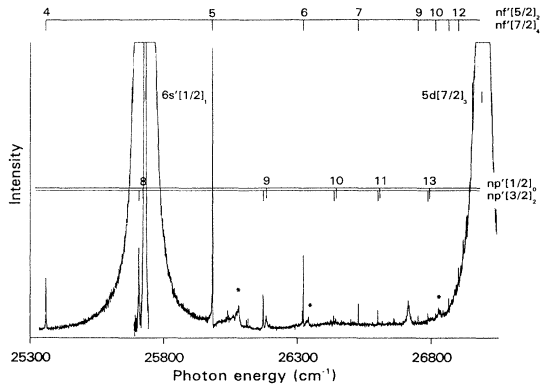


FIG. 4. Four-photon excitation spectrum of autoionizing series in Xe between the $^2P_{3/2}$ and $^2P_{1/2}$ ionic limits obtained with linearly polarized excitation light.

Resonances belonging to the $nf'[5/2]_2$ and $nf'[7/2]_4$ series can be observed up to $n=12$. For the lowest members of these series, viz., $4f'[5/2]_2$ and $4f'[7/2]_4$, the difference in excitation energy is just large enough so that they can be resolved with linearly polarized excitation light. Using circularly polarized light the signal attributed to the $4f'[5/2]_2$ state has disappeared completely, while the $4f'[7/2]_4$ resonance has an increased intensity (Fig. 5). For the higher members of the $nf'$ series the resonances of the $J=2$ and 4 components cannot be resolved under linearly polarized excitation conditions. When the polarization was changed from linear to circular a small shift of the resonances was observed, indicating that the $nf'[5/2]_2$ and $nf'[7/2]_4$ states have slightly different excitation energies, similar to what was observed in Kr. The ratios $S_{\text{lin}}/S_{\text{cir}}$ for the observed members of the series in Xe are given in Table I.

The two large resonances at one-photon energies of 25 728 and 26 990 $\text{cm}^{-1}$, which result from the (3+1) REMPI signals of the $6s'[1/2]_1$ and $5d[7/2]_3$ states, are seen to be heavily broadened by power effects. When the laser power was reduced, the broadening decreased and the $8p'[3/2]_2$ resonance could be observed, though the other component $8p'[1/2]_0$ still overlapped with the strong (3+1) REMPI signal of the $6s'[1/2]_1$ state. As in Kr, the $8p'[3/2]_2$ resonance can be observed at much lower laser powers than those necessary for the other members of the $np'$ series. It can therefore be concluded that the cross section of this state is much larger that those of the other members of the series.

The broad signals observed in Fig. 4 at one-photon energies of 26 083, 26 343, and 26 831 $\text{cm}^{-1}$, marked with

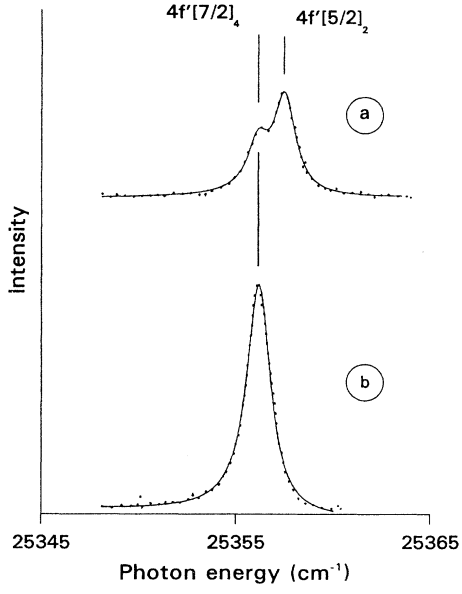


FIG. 5. High-resolution four-photon excitation spectrum of the $4f'[5/2]_2$ and $4f'[7/2]_4$ autoionizing resonances in Xe. (a) Four-photon excitation spectrum using linearly polarized excitation light. (b) Four-photon excitation spectrum using circularly polarized excitation light.

asterisks, are probably due to autoionizing resonances of xenon dimers. Additionally, an unidentified broad signal is observed at a one-photon energy of 26 717 $cm^{-1}$, which overlaps with the $12p'[1/2]_0$, $12p'[3/2]_2$, $8f'[5/2]_2$, and $8f'[7/2]_4$ autoionizing resonances.

## IV. DISCUSSION

In the preceding section the results of a multiphoton ionization study of even autoionizing states of the atoms Ar, Kr, and Xe between their $^2P_{3/2}$ and $^2P_{1/2}$ ionic limits by means of four-photon excitation have been presented. Excitations have been performed using both linearly and circularly polarized excitation light, allowing for a detailed investigation of these autoionizing states. In this section we shall analyze the line shapes of the resonances using a line-shape formula derived by Ueda [21] and discuss the polarization dependence of resonance intensities. The analysis of the resonance line shapes results in a set of line-shape parameters, which enable a quantitative description of the profiles and a comparison with previously obtained experimental and theoretical data. Finally, the qualitative differences between the four-photon excitation spectra of the three rare gases will be discussed.

### A. Parametrization of the autoionizing resonances

A complete analysis of the spectra obtained in the present study would be preferably performed from first principles using a complete multichannel quantum-defect theory approach [22–30]. Since such a treatment is rather involved, it will not be pursued in the present study. Instead, the line shapes of the resonances will be analyzed in a similar way as done in our study of the odd autoionizing states of Ar, Kr, and Xe using three-phonon excitation, i.e., using the line-shape formula derived by Ueda [21] under the assumption of negligible closed-channel interactions

$$\sigma(E)=\sigma_{nc}+\sum_l \sigma_{rc,l}(q_l+\epsilon_l)^2/(1+\epsilon_l^2) \ . \tag{1a}$$

Here $\sigma_{rc,l}$ represents the cross section for the transition to the open channel which interacts with the closed channel $l$, $\sigma_{nc}$ the cross section of the noninterfering continuum, $q_l$ the asymmetry parameter, and $\epsilon$ a periodic energy scale given by

$$\epsilon_l=\tan[\pi(\nu_{1/2}+\mu_l)]/W_l \ , \tag{1b}$$

$$\nu_{1/2}=[R/I_{1/2}-E]^{1/2} \ . \tag{1c}$$

Here $\mu_l$ represents the quantum defect, $W_l$ the width parameter, $R$ the mass-corrected Rydberg constant, $I_{1/2}$ the second ionization limit, and $E$ the four-photon energy of interest.

For relatively narrow resonances ($W \ll 1$), the quantum defect $\mu_l$ and width parameter $W_l$ are related to the resonance energy $E_n$ and resonance width $\Gamma_n$ by the relations [21,4]

$$I_{1/2}-E_n=R/(n-\mu_l)^2 \ , \tag{2a}$$

$$\Gamma_n/2=2RW_l/\pi(n-\mu_l)^3 \ . \tag{2b}$$

The parameters $\mu_l$, $W_l$, $q_l$, $\sigma_{nc}$, and $\sigma_{rc,l}$ are, to a first approximation, independent of the energy and can be related to MQDT parameters under the stringent assumption of negligible closed-channel interactions. As has been shown by Ueda [21,30] and extensively discussed in our previous study [15], the parameters $\mu_l$ and $W_l$ are, under this assumption, independent of the excitation scheme.

Since no calculations have been performed on the four-photon excitation spectra of autoionizing states between the two lowest ionic limits of rare gases, we cannot compare our results directly to theoretical data. However, calculations in which the two-photon excitation spectra to the same energy region were considered have been performed [29]. Since the excitation scheme in these calculations is different from the excitation scheme used in the present study, the calculated and experimental spectra cannot be compared in detail. Parametrization of the experimental and theoretical results using the line-shape formula, however, enables the quantum defects $\mu_l$ and width parameters $W_l$ to be compared. As mentioned above, under the assumption of negligible closed-channel interactions these parameters are not dependent on the excitation scheme. The line-shape parameters of the resonances observed in the experimental spectra have been obtained by fitting the experimental spectra with the line-shape formula, while the theoretically predicted $\mu_l$ and $W_l$ parameters have been determined from the calculated MQDT parameters using complex quantum defects defined by Seaton [30,31].

### B. Relative intensities of a four-photon transition

The transition amplitude of a four-photon excitation from an initial state $g$ to a final state $f$ is proportional to [28]

$$\sigma_{fg} \sim \sum_{a_1,a_2,a_3} \frac{\langle f|\mathbf{r}\cdot\boldsymbol{\epsilon}|a_3\rangle\langle a_3|\mathbf{r}\cdot\boldsymbol{\epsilon}|a_2\rangle\langle a_2|\mathbf{r}\cdot\boldsymbol{\epsilon}|a_1\rangle\langle a_1|\mathbf{r},\boldsymbol{\epsilon}|g\rangle}{[E_{a_3}-E_g-3h\nu][E_{a_2}-E_g-2h\nu][E_{a_1}-E_g-h\nu]} \ . \tag{3}$$

Here $h\nu$ represents the photon energy, $\epsilon$ the polarization direction of the laser light, $a_i$ all intermediate states, and $E_{ai}$ the energy of state $a_i$. Equation (3) shows that the four-photon transition probability contains a summation of the contributions of all possible excitation routes. The weight of each route is dependent on the dipole transition moments and the energy differences between the one-, two-, and three-photon energy levels and the excitation

energies of the states $a_i$. The dipole transition moments are dependent on the electronic characters of the states involved and on the polarization of the excitation light.

Generally, many states are involved in a multiphoton transition. Interferences between all the different contributions will finally determine the total cross section. If, however, a virtual level is near resonance with a real state, one energy term in the denominator will almost vanish and the contributions of some excitation routes can become very large. As a consequence, the total cross section, which will then mainly consist of the contributions of excitation routes in which this near-resonance state is involved, can be strongly enhanced [32].

If the weight factors determined by the energy differences given in Eq. (3) are examined for the four-photon transitions described in the present study, near-resonance effects can be expected at the three-photon virtual level. Excitation routes in which the lowest members of the $ns'[1/2]_1$ series are involved can have large influences on the total cross section. The one- and two-photon virtual levels are, in the present study, far from resonance and their influence on the cross section is expected to be largely independent of the photon energy.

In the present study the autoionizing states are excited using linearly and circularly polarized excitation light. By changing the polarization from linear to circular, the four-photon nonresonant transitions to $J=0$ and 2 states become forbidden, while the intensities of $J=4$ states should theoretically increase by a factor $\frac{35}{8}$ [33]. The relative contributions of the two components $J=2$ and 4 to the unresolved $nf'$ resonances observed with linearly polarized excitation light is then given by

$$S_{J=2}/S_{J=4}=\tfrac{35}{8}(S_{\text{lin}}/S_{\text{cir}})-1 \ . \tag{4}$$

Here $S_{\text{lin}}$ is the total signal intensity of the signal comprised of the unresolved $nf'[5/2]_2$ and $nf'[7/2]_4$ resonances using linearly polarized excitation light, while $S_{\text{cir}}$ is the total signal intensity using circularly polarized light.

The factor $\frac{35}{8}$ used in Eq. (4) is defined for a truly nonresonant four-photon transition [33]. The $4f'$ resonances in Xe could be used to check this value for a transition in which near resonances might be important, since in this atom the two components $4f'[5/2]_2$ and $4f'[7/2]_4$ could be resolved using linearly polarized excitation light. From the ratio $S_{J=2}/S_{J=4}$, which is deduced from the spectrum measured with linearly polarized light [Fig. 5(a)], and $S_{\text{lin}}/S_{\text{cir}}$ [Figs. 5(a) and 5(b)], a factor of 4.37(0.4) was obtained. This factor agrees very well with the theoretical value $\frac{35}{8}$ (4.375). We can therefore conclude that near-resonance effects do not seem to influence this factor significantly. In order to deduce the ratio $S_{J=2}/S_{J=4}$ for all other $nf'$ resonances observed in the present study, it was therefore assumed that the theoretical value of $\frac{35}{8}$ could be used throughout.

### C. Argon

In Ar the resonances deriving from the $np'[1/2]_0$ and $np'[3/2]_2$ series could not be resolved, in contrast to what was observed for Kr and Xe (see Fig. 2). As to why these two components are not resolved in Ar, two reasons can be put forward. First, the members of the $np'[1/2]_0$ and $np'[3/2]_2$ series located above the $^2P_{3/2}$ ionic limit have principal quantum numbers $n^*=n-\mu\geq 9.4$, 5.4, and 3.4 for Ar, Kr, and Xe, respectively. The energy splitting between the lowest autoionizing members of these two series, which decreases for larger $n^*$, is therefore smaller as the atom gets lighter. Second, in the experiments on Ar frequency-doubled laser light was used, which has an inherently larger bandwidth than the fundamental light used in the experiments on Kr and Xe. Since the two components are not resolved, no detailed analysis of the resonances can be performed. Only the energies of the maxima of the resonances and the total width of the resonance line can be determined. Assuming that the $np'$ resonances for the different atoms show similar resonance line shapes, which is corroborated by our observations in Kr and Xe (Fig. 2), the maxima can be correlated to the maxima of the sharp $np'[3/2]_2$ resonances. The quantum defects for this series obtained from these excitation energies using Eq. (2a) are given in Table II. The analysis of the line shapes of the unresolved resonances in terms of a single line-profile results in a width parameter $W=0.29(0.004)$ after correction for the laser bandwidth.

The results of the line-shape analysis of the narrow resonances of the $nf'$ series are given in Tables II–IV. The quantum defects of the resonances are very small, as would be expected for series with a large electronic angu-

TABLE II. Line profile parameter $q_l$ obtained for the $np'[1/2]_0$, $np'[3/2]_2$, $nf'[5/2]_2$, and $nf'[7/2]_4$ autoionizing series in Ar, Kr, and Xe from the analysis of four-photon excitation spectra by means of Eq. (1).

| | $np'[1/2]_0$ | $np'[3/2]_2$ | $nf'[5/2]_2$ | $nf'[7/2]_4$ |
|---|---|---|---|---|
| Ar | | | $n=10$–$11$:large negative | $n=10$–$11$:large negative |
| Kr | $n=8$:11(5) | $n=8$:23(10) | $n=7$–$10$:large negative | $n=7$–$10$:large negative |
| | $n=9$:6(3) | $n=9$:14.5(6) | | |
| | $n=10$:3.5(1) | $n=10$:6.7(3) | | |
| | $n=11$:3.4(1) | $n=11$:4.7(2) | | |
| Xe | | $n=8$:100(80) | $n=5$–$7$:large negative | $n=4$–$7$:large negative |
| | $n=9$:3(1) | $n=9$:30(20) | | |
| | $n=10$:2.8(1) | $n=10$:19(10) | | |
| | $n=11$:1.8(1) | $n=11$:14(7) | | |

lar momentum, and the variations between the quantum defects of the various members are negligible. After correction for the laser bandwidth the width parameters of the resonances are determined as $W=0.0059(0.002)$. By changing the polarization of the excitation light, the intensity of the resonances changed, while the other line-shape parameters remained the same. From the ratio $S_{\text{lin}}/S_{\text{cir}}$ the contributions of the $nf'[5/2]_2$ and $nf'[7/2]_4$ resonances could be established using Eq. (4) and are given in Table I. From this table it can be concluded that the $nf'$ resonances measured with linearly polarized light have a major contribution from the $nf'[5/2]_2$ state. Our observation that the line-shape parameters are similar under both circularly and linearly polarized excitation conditions indicates that the excitation energies of the $nf'[5/2]_2$ and $nf'[7/2]_4$ resonances are almost identical. Since the even autoionizing states of Ar have not been observed before and since no theoretical calculations have been performed on these states, a comparison with other data is not possible.

For an unperturbed series the *peak* intensities of different members of one series under nonresonant excitation conditions are expected to be constant in first approximation, though their *integrated* intensities will fall off with $n^{*-3}$ as a result of the decreasing line width as a function of $n^*$. In contrast, the excitation spectrum of Ar shows that the peak intensities of the $np'$ resonances decrease strongly for increasing values of $n$. The observation of a strong energy dependence of the cross section in a series can be explained by strong perturbations of the autoionizing states or by near-resonance effects in the excitation mechanism. Such near-resonance effects are indeed expected to be important, as the three-photon virtual level is close to the $4s'[1/2]_1$ state located at 95 400

TABLE III. Quantum defects $\mu_l$ obtained for the $np'[1/2]_0$, $np'[3/2]_2$, $nf'[5/2]_2$, and $nf'[7/2]_4$ autoionizing series in Ar, Kr, and Xe. (a) Quantum defects obtained from the present experimental results from the analysis of the four-photon excitation spectra by means of Eq. (1). (b) Quantum defects at the ionic limits $I_{3/2}$ and $I_{1/2}$ are given as calculated by complex quantum-defect theory from the results of previous MQDT calculations.

| | $np'[1/2]_0$ | $np'[3/2]_2$ | $nf'[5/2]_2$ | $nf'[7/2]_4$ |
|---|---|---|---|---|
| | | (a) Present experimental results | | |
| Ar | | $n=11$–$20$:1.614(0.008) | $n=10$–$15$:0.010(0.005) | $\mu_{nf'[5/2]_2}$ |
| Kr | $n=8$:2.569(0.003) | $n=8$:2.619(0.003) | $n=5$:0.0132(0.003) | $\mu_{nf'[5/2]_2}+0.0006$ |
| | $n=9$:2.558(0.004) | $n=9$:2.610(0.004) | $n=6$:0.0089(0.004) | |
| | $n=10$:2.553(0.006) | $n=10$:2.605(0.006) | $n=7$:0.0109(0.005) | |
| | $n=11$:2.544(0.009) | $n=11$:2.597(0.009) | $n=8$:0.0016(0.006) | |
| | $n=12$:2.534(0.011) | $n=12$:2.587(0.011) | $n=9$:−0.0009(0.010) | |
| | $n=13$:2.508(0.014) | $n=13$:2.573(0.014) | $n=10$:−0.0130(0.015) | |
| | $n=14$:2.500(0.020) | $n=14$:2.555(0.020) | $n=11$:−0.0268(0.020) | |
| | $n=15$:2.487(0.026) | $n=15$:2.551(0.026) | $n=12$:−0.0408(0.025) | |
| | | | $n=13$:−0.0526(0.030) | |
| | | | $n=14$:−0.0677(0.036) | |
| | | | $n=15$:−0.0808(0.045) | |
| | | | $n=16$:−0.1161(0.060) | |
| | | | $n=17$:−0.1178(0.070) | |
| | | | $n=18$:−0.1341(0.090) | |
| | | | $n=19$:−0.1735(0.10) | |
| | | | $n=20$:−0.2013(0.12) | |
| | | | $n=21$:−0.2375(0.15) | |
| Xe | $n=7$:3.533[a] | $n=7$:3.565[a] | $n=4$:0.0239(0.003) | $\mu_{nf'[5/2]_2}+0.0020$ |
| | $n=8$:- | $n=8$:3.551(0.002) | $n=5$:0.0276(0.003) | |
| | $n=9$:3.511(0.003) | $n=9$:3.542(0.003) | $n=6$:0.0305(0.003) | |
| | $n=10$:3.507(0.004) | $n=10$:3.537(0.004) | $n=7$:0.0283(0.006) | |
| | $n=11$:3.500(0.006) | $n=11$:3.530(0.006) | $n=9$:0.0271(0.010) | |
| | $n=13$:3.499(0.009) | $n=13$:3.527(0.009) | $n=10$:0.0254(0.012) | |
| | $n=18$–$31$:3.495(0.008)[b] | | $n=11$:0.0365(0.015) | |
| | | | $n=12$:0.0165(0.020) | |
| | | (b) Theoretical results[c] | | |
| Ar | | | | |
| Kr | $I_{3/2}$:2.559 | $I_{3/2}$:2.635 | $I_{3/2}$:0.0088 | |
| | $I_{1/2}$:2.543 | $I_{1/2}$:2.634 | $I_{1/2}$:0.0053 | |
| Xe | $I_{3/2}$:3.557 | $I_{3/2}$:3.608 | $I_{3/2}$:0.0259 | |
| | $I_{1/2}$:3.543 | $I_{1/2}$:3.601 | $I_{1/2}$:0.0239 | |

[a]Obtained from [9].
[b]Obtained from [10].
[c]Obtained from [29].

TABLE IV. Width parameters $W_l$ obtained for the $np'[1/2]_0$, $np'[3/2]_2$, $nf'[5/2]_2$, and $nf'[7/2]_4$ autoionizing series in Ar, Kr, and Xe. (a) Width parameters obtained from the present experimental results from the analysis of the four-photon excitation spectra by means of Eq. (1). (b) Width parameters at the ionic limits $I_{3/2}$ and $I_{1/2}$ are given as calculated by complex quantum-defect theory from the results of previous MQDT calculations.

| | $np'[1/2]_0$ | $np'[3/2]_2$ | $nf'[5/2]_2$ | $nf'[7/2]_4$ |
|---|---|---|---|---|
| | | (a) Present experimental results | | |
| Ar | $n=11-13$:0.029(0.004) | | $n=10$:0.0059(0.002) | $W_{nf'[5/2]_2}$ |
| Kr | $n=8-10$:0.029(0.005) | $n=8-10$:0.0077(0.003) | $n=5-7$:0.0050(0.002) | $Wnf'_{[5/2]_2}$ |
| Xe | $n=9-12$:0.028(0.004) | $n=9-12$:0.0095(0.004) | $n=4-5$:0.0029(0.001) | $W'_{[5/2]_2}$ |
| | | (b) Theoretical results[a] | | |
| Ar | | | | |
| Kr | $I_{3/2}$:0.026 | $I_{3/2}$:0.011 | $I_{3/2}$:0.000 | |
| | $I_{1/2}$:0.028 | $I_{1/2}$:0.013 | $I_{1/2}$:0.000 | |
| Xe | $I_{3/2}$:0.022 | $I_{3/2}$:0.013 | $I_{3/2}$:0.002 | |
| | $I_{1/2}$:0.020 | $I_{1/2}$:0.014 | $I_{1/2}$:0.002 | |

[a]Obtained from [29].

$cm^{-1}$. As a result of this near resonance the cross sections of the $np'$ resonances might be enhanced, as was discussed in Sec. IV B. If the enhancement should be attributed to near resonance with the $4s'[1/2]_1$ state, then it should decrease as the energy difference between the virtual three-photon level and the $4s'[1/2]_1$ state increases. Since this is exactly what is observed in the excitation spectrum, we conclude that the observed strong energy dependence of the cross section of these series should be attributed to near-resonance effects.

The peak intensities of the $nf'$ resonances are observed to change somewhat in going from the first to the second ionic limit. The main reason for these changes is found in the fact that the widths of these resonances become smaller than the excitation bandwidth for higher members of these series. Taking this into account, we can conclude that the excitation mechanism for the transitions to the $nf'$ states is probably not as strongly influenced by near-resonance effects at the three-photon level as is observed for the $np'$ resonances. This is indeed to be expected when selection rules are considered. In a four-photon excitation process to the $np'$ resonances excitation routes, which involve states with $s'$ character at the three-photon level, can contribute to the total cross section and near-resonance effects caused by the $4s'[1/2]_1$ state might be expected. In a four-photon excitation process to the $nf'$ states, on the other hand, enhancement by $s'$ character at the three-photon level is not allowed and near-resonance effects caused by the $4s'[1/2]_1$ state are expected to be considerably smaller.

### D. Krypton

In the present study Kr was excited to $np'[1/2]_0$, $np'[3/2]_2$, $nf'[5/2]_2$, and $nf'[7/2]_4$ autoionizing states between the two lowest ionic limits. Four-photon excitation of such autoionizing states has been studied previously by Blazewicz *et al.* [16] and Proctor *et al.* [17], who reported, however, only a limited number of resonances. In our experiments, on the other hand, the complete energy region between the two lowest ionic limits was investigated using both linearly and circularly polarized excitation light, enabling a much more complete and accurate description of the autoionizing states and of the excitation mechanisms.

Our results differ in a number of aspects from those of previous studies. First, the energy resolution in our experiments is superior, allowing the two components of the $np'$ resonances to be observed separately. Second, in the previous studies the resonance structures were superimposed on a nonresonant background ionization signal, while in our spectra this background is considerably smaller. Finally, it was found previously that the line shapes of the $nf'$ resonances were strongly dependent on the gas pressure. We notice that these experiments have been performed in a cell, while we used a supersonic expansion. It has been suggested that third-harmonic generation (THG) was responsible for the changes in the resonance line profiles as a function of the gas pressure. In the present study the role of THG was thoroughly investigated and it was found that the pressure effects on the excitation spectra appeared to be minimal. Another indication that THG is not important in the present study is found in our measurements with circularly polarized excitation light. Under such conditions THG is forbidden. The ratios of the signal intensities, measured with linearly and circularly polarized light as a function of pressure, can therefore be used to investigate the influence of THG. Since these ratios did not depend on pressure, we conclude that the role of THG in the present experiments is negligible.

The resonances observed in the present study were analyzed by means of the line-shape formula given in Eq. (1). The results of this analysis are given in Tables II–IV. It was found that Eq. (1) provides an excellent description of the autoionizing profiles as can be seen, e.g., in Fig. 2(b). In this figure the measured $10p'[1/2]_0$ and $10p'[3/2]_2$ resonances are shown together with a fit

based on Eq. (1), which consists in this case of the summation of two independent line profiles.

When we consider the quantum defects of various members of the $np'[1/2]_0$, $np'[3/2]_2$, $nf'[5/2]_2$, and $nf'[7/2]_4$ series as derived from the fits, it is observed that they are not constant as would be expected. Especially for the higher members of each series a strong decrease in the quantum defects is seen. These quantum defects result from fits in which the ionization energy of the $^2P_{1/2}$ ionic limit is fixed at the literature value (118 284.5 $cm^{-1}$) [34]. If, on the other hand, the observed resonance energies of the members of the various series are fitted to the standard Rydberg formula with both quantum defect and ionization energy treated as fit parameters, it turns out that the various series can be fitted quite well (see Table V). An intriguing aspect of these fits is, however, that the fitted values of the ionization energy (118 296, 118 295, and 118 291 $cm^{-1}$ for the $np'[1/2]_0$, $np'[3/2]_2$, and $nf'$ series, respectively) differ significantly from the literature value. Also in the experiments of Blazewicz *et al.* [16] the analysis of the resonance energies of the members belonging to the $nf'$ series resulted in a value for the ionization energy (118 295 $cm^{-1}$), which was considerably higher than the established value.

A possible explanation for the obvious failure to reproduce the ionization energy of the $^2P_{1/2}$ ionic limit in Kr correctly might be found in the ac Stark effect. This would cause a shift and broadening of the resonances [35] and would ultimately result in an ionization energy which would appear too high. Indeed, we found in our experiments that the resonances are shifted to higher energies as the power was increased and that the widths of the resonances are strongly susceptible to laser power. Such an ac Stark effect would also nicely explain the difference in the ionization energies derived from the resonance energies of the members of the $nf'$ series in our study (118 291 $cm^{-1}$) and in the study of Blazewicz *et al.* [16] (118 295 $cm^{-1}$), since in the latter study considerable higher laser powers have been used.

From the above it becomes clear that ideally one would wish to correct the line-shape parameters and resonance positions for the ac Stark effect by a systematic study of the dependence of these parameters on the laser power. In our experiments, however, a sufficient signal could only be obtained for a small range of laser powers and only for a limited number of resonances. The results of such an analysis for the relatively strong $8f'$ resonance are given in Fig. 6. From this figure it can be observed that the resonance energy is shifted to higher energy and that the line shape is broadened when the laser power is increased. Both the resonance position and the width of the resonance show a clear linear dependence on laser power. From the figure it can also be concluded that the resonance measured at the lowest possible laser power is still influenced by the ac Stark effect.

The ionization energy determined previously from the positions of the $nf'$ resonances at minimal laser power using the standard Rydberg formula was found to be 6 $cm^{-1}$ above the literature value. From an extrapolation of the power dependence of the $8f'$ resonance, on the other hand, we find the ac Stark shift at the minimal laser power to be about 2 $cm^{-1}$, thereby not accounting completely for the difference of 6 $cm^{-1}$. For the two components of the $10p'$ resonance a similar analysis was performed. This analysis shows qualitatively the same behavior, as found for the $nf'$ resonances. For these resonances the fitted ionization energy using the standard Rydberg formula was 11 $cm^{-1}$ higher than the literature value, whereas the ac Stark shift for the resonances at minimal laser power for which resonance positions were determined was about 5 $cm^{-1}$. Apparently the high ionization energy determined from the fits cannot be completely attributed to ac Stark effects.

As outlined in the experimental section, the signal intensities of the lowest autoionizing members of the $np'$ series are much larger than those of the higher members. These differences in peak intensities are undoubtedly due to near-resonance effects at the three-photon level caused by the lowest $ns'[1/2]_1$ excited state, viz., $5s'[1/2]_1$ similar to what was observed for the $np'$ resonances in Ar. The signal intensities of the members of the $nf'$ resonances, on the other hand, would at first seem to indicate that such near-resonance effects are not important for these series. The peak intensities shown in Fig. 3 were

TABLE V. Ionization energies and quantum defects as obtained by fitting the excitation energies of the members of the $np'[1/2]_0$, $np'[3/2]_2$, and $nf'$ series with the standard Rydberg formula [Eq. (2a)].

| Series | $I_{1/2}$ ($cm^{-1}$) | $\mu_l$ |
|---|---|---|
| $np'[1/2]_0$ | 118 296.16(2.3) | 2.576(0.0036) |
| $np'[3/2]_2$ | 118 294.74(1.9) | 2.625(0.003) |
| $nf'$ | 118 290.80(1.1) | 0.0167(0.0020) |
| $nf'$[a] | 118 295(2) | 0.021 |

[a]Obtained in [16].

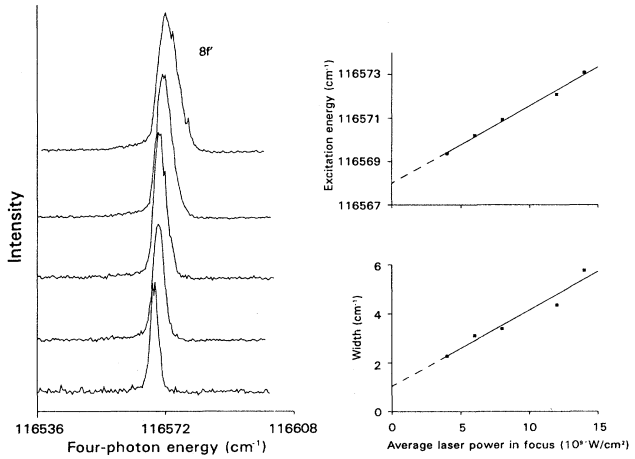


FIG. 6. On the left, excitation spectra of the $8f'$ resonances in Kr are shown measured at different laser powers. On the right, the excitation energy and the full width at half maximum of those resonances are shown as a function of the laser intensity.

not corrected for the laser power. As a consequence, differences in peak intensities would only be significant if the peak intensities would differ appreciably, as was the case for the different members of the $np'$ series. As will become clear from the analysis of the ratios of the signal intensities of the $nf'$ resonances measured with linearly and circularly polarized light ($S_{\text{lin}}/S_{\text{cir}}$), near-resonance effects do influence, however, the relative peak intensities of the $nf'$ resonances. From these ratios the relative contributions of the $nf'[5/2]_2$ and $nf'[7/2]_4$ states to the resonance signal measured with linearly polarized light ($S_{J=2}/S_{J=4}$) were obtained by means of Eq. (4) (Table I). It should be emphasized that these experimental ratios are independent of laser power and therefore allow for a direct comparison of the various members. Table I shows that the ratio $S_{J=2}/S_{J=4}$ increases monotonically from 4.25 for the $9f'$ resonance to 6.39 for the $6f'$ resonance, while for the $5f'$ resonance a ratio of 2.02 was found. Apparently, the relative four-photon cross section of the $J=2$ and 4 components of the $nf'$ resonances changes for excitation to different members of these series.

A logical candidate for a state which might be involved in the near-resonance effects at the three-photon virtual level is the $5s'[1/2]_1$ state. The observed changes in the ratio $S_{J=2}/S_{J=4}$ for the various members would be in line with such an assumption. The ratio $S_{J=2}/S_{J=4}$ changes smoothly when going from the $n=6$ member to higher members of the $nf'$ series. Since the energy differences between the three-photon energy and the near-resonance state only change in magnitude, such a regular trend of the ratio $S_{J=2}/S_{J=4}$ would be expected. For the excitation to the $5f'$ autoionizing state not only the magnitude, but also the sign of the energy difference between the three-photon level and the $5s'[1/2]_1$ state changes. The result of interference between different contributions to the total cross section for this member is therefore expected to be quite different from that of the other members. This is indeed what is observed.

From four-photon excitation selection rules it can be concluded that the $5s'[1/2]_1$ state cannot be involved at the three-photon virtual level in ($J=4 \leftarrow J=0$) excitations and thus cannot cause near-resonance effects on the cross section in the excitations to $nf'[7/2]_4$ states. Differences in the ratio $S_{J=2}/S_{J=4}$ for the various members of the $nf'$ series are therefore due to the change in signal intensity of the $J=2$ component rather than of the $J=4$ component. The same selection rules would also prohibit that the near-resonance effects result from the main electronic character of the $5s'[1/2]_1$ state, i.e., $s'$ character. Rather it should be some $d(J=1)$ or $d'(J=1)$ electronic character mixed into the $5s'[1/2]_1$ state, which is responsible for the near-resonance effects. Perturbations of the $5s'[1/2]_1$ state, which have already been extensively investigated in previous studies [2], thus seem to play a key role in the four-photon excitations of the $nf'$ autoionizing resonances in Kr.

Near-resonance effects, which were shown above to be of considerable importance in explaining the resonance intensity changes, also become apparent in the $q$ parameters of the $np'$ resonances. As shown in Table II, the $q$ parameters, for which larger values are found for resonances of the $np'[3/2]_2$ component than those of the $np'[1/2]_0$ component, decrease as $n$ increases. Since the $q$ parameter is directly related to the cross section of the autoionizing state, which differs for the various members of one series due to near-resonance effects, somewhat different resonance profiles of members of one series might indeed be expected. The $nf'$ resonances are nearly symmetric and the $q$ parameter is therefore very large, as found in Ar. These parameters do not show any clear dependence on the principal quantum number. It should be borne in mind, however, that differences in the $q$ parameter of resonances which are nearly symmetric ($|q|>10$) are difficult to determine with the present signal-to-noise ratios and small variations in $q$ might not be observed.

In Tables III and IV a comparison is made between line-shape parameters as determined in the present study with those of previous theoretical studies [29]. The quantum defects of the *lower* members of each series are expected to be only affected to a minor extent by ac Stark effects. Taking these values as experimental results, reasonable agreement is found with the calculated quantum defects. Above we found that the widths of the resonances are also susceptible to power effects. The width parameters for the resonances determined from the line-shape analyses could therefore be slightly too large. Theoretical predictions of the width parameters seem to be in reasonable agreement with experimental results for the $np'[1/2]_0$ series, while those of $np'[3/2]_2$ series seem to be slightly overestimated.

### E. Xenon

Autoionizing states between the two lowest ionic limits of Xe have previously been investigated by Blazewicz *et al.* [16], who obtained four-photon excitation spectra using linearly polarized excitation light. The experimental results of this study are in reasonable agreement with the present results, although some differences caused by different experimental conditions can be noticed. First, our experiments were performed with a higher resolution, allowing the $J=0$ and 2 components of the $np'$ states to be resolved up to $n=13$ and enabling a detailed analysis of the line shapes of all observed resonances. Second, our spectra show some broad features, which are attributed to dimers. As might be expected, these features have not been observed in the experiments of Blazewicz *et al.* [16], since their experiments have been performed in a cell. Finally, in the present study four-photon excitation of the autoionizing states, in particular the $nf'$ states, was performed using both linearly and circularly polarized excitation light, allowing for a detailed analysis of these resonances and the excitation mechanism.

The results of the line-shape analyses on the basis of Eq. (1) are given in Tables II–IV. The quantum defects of the members of the $np'$ series are not constant, in contrast to *a priori* expectations. An analysis of the quantum defects shows a linear energy dependence. It should be emphasized that this nonconstant behavior of the quantum defects is quite different from the behavior which was found for the quantum defects in Kr. In Kr the

quantum defects were observed to change strongly for higher members as a result of power effects. The resonances in Xe do not show such a susceptibility to the laser intensity, though we hasten to notice that a power dependence could only be studied for an even smaller range of laser intensities than in Kr. Further corroboration that the quantum defect indeed is linearly dependent on the excitation energy is found in the quantum defects of lower and higher members than the ones observed in the present study. The lowest autoionizing members of the $np'$ series, i.e., the $7p'[1/2]_0$ and $7p'[3/2]_2$ states, could not be observed in our experiments, since not enough laser power could be generated at the appropriate wavelength, while the members with $n > 13$ could not be observed using the present excitation scheme, because they overlap with the huge (3+1) REMPI signal of the $5d[7/2]_3$ state. From previous studies of Grandin and Husson [9] and Ernst, Softley, and Zare [18] in which different excitation schemes have been used, the excitation energies of the $7p'[1/2]_0$, $7p'[3/2]_2$, and $(18-31)p'[1/2]_0$ are well known. If the quantum defects of these members are also taken into account, a linear energy dependence of the quantum defects of the members of the two $np'$ series comes out clearly, as is shown in Fig. 7. We therefore conclude that the nonconstant behavior of the quantum defects is an intrinsic property of these Rydberg series and does not result from ac Stark effects.

The quantum defects determined for the $nf'$ resonances are quite constant. In a previous study Grandin and Husson [9] have measured accurate excitation energies for the lowest members of this series, i.e., $4f'[5/2]_2$ and $5f'[5/2]_2$. The resonance energies of these states obtained in the present experiments agree very well with their results, indicating that shifts caused by power effects as observed in Kr are negligible.

The $q$ parameters of the $np'$ resonances show much resemblance to those found for the same series in Kr. The $q$ parameters of the $J=2$ components are larger than those of the $J=0$ components and the $q$ parameter values

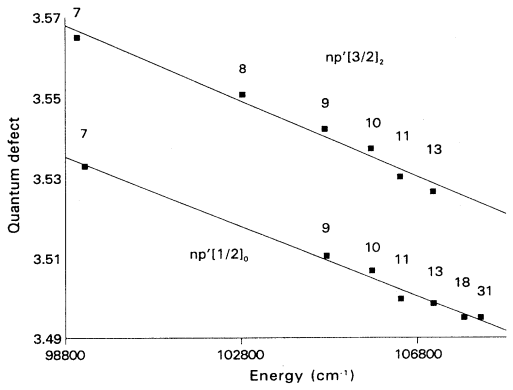


FIG. 7. Quantum defect of the members of the $np'[1/2]_0$ and $np'[3/2]_2$ series in Xe as a function of the excitation energy. The quantum defects of the $7p'[1/2]_0$, $7p'[3/2]_2$, and $(18-31)p'[1/2]_0$ resonances have been obtained from [9] and [18].

of members belonging to one series decrease as $n$ increases. Again, near-resonance effects are probably the origin of these differences between the various members. For the $nf'$ resonances similar $q$ parameters were obtained as for Ar and Kr.

In our experiments on Ar and Kr it was observed that the peak intensities of the lower members of the $np'$ series were considerably stronger than those of the higher members. Also for Xe this trend in peak intensities is found and can be attributed to the near-resonance effects at the three-photon virtual level caused by lowest $ns'[1/2]_1$ state, viz., $6s'[1/2]_1$. As has been discussed in the case of Kr, this near-resonance state can also influence the four-photon excitation cross sections of the $nf'[5/2]_2$ states. However, again the $d$ or $d'$ character mixed into this state and not the dominant electronic $s'$ character of the $6s'[1/2]_1$ state is involved.

The ratios $S_{J=2}/S_{J=4}$ of the $nf'$ resonances determined from the ratios $S_{\text{lin}}/S_{\text{cir}}$ are given in Table I. These ratios, which differ strongly for the various members, indicate that also in the four-photon excitation to the $nf'[5/2]_2$ states in Xe near-resonance effects are important. The trends in the ratio $S_{J=2}/S_{J=4}$ are quite similar to what was found for Kr. $S_{J=2}/S_{J=4}$ increases monotonically as $n$ decreases, as long as the three-photon energy is above the excitation energy of the lowest $s'[1/2]_1$ state. If, however, the three-photon energy becomes lower than the excitation energy of this state, which is the case for the $4f'$ resonance, the ratio $S_{J=2}/S_{J=4}$ strongly decreases as can be seen from Table I.

The quantum defects and width parameters determined from our experiments can be compared with those obtained from the MQDT parameters calculated in theoretical studies [29] (see Tables III and IV). The largest differences between theory and experiment are found in the quantum defects of the $np'[1/2]_0$ and $np'[3/2]_2$ series, which are overestimated in the calculations. Possibly, this difference is connected with the experimentally observed linear energy dependence of the quantum defect. This might indicate that the members of these series are perturbed and consequently more difficult to describe accurately. The resonances might be slightly broadened by power effects. Width parameters determined from experimentally observed resonances might therefore be slightly too large. Taking this into account, the theoretical and experimental width parameters of the $np'[1/2]_0$ series seem to be in reasonable agreement. As in Kr, the width parameter of the $np'[3/2]_2$ series is slightly overestimated by the theoretical calculations.

### F. Influences of the three-photon virtual level

In the previous sections we have analyzed the four-photon excitation spectra of the rare gases Ar, Kr, and Xe individually. From these analyses it has become clear that the four-photon ionization dynamics are to an appreciable extent influenced by the electronic characteristics of the three-photon virtual level. In this section it will be shown that on the basis of a comparison of the three-photon virtual levels in these three rare-gas atoms we can

rationalize the observed differences between their four-photon excitation spectra.

In the present experiments the influence of the three-photon virtual level is mainly determined by two aspects. The first concerns the energy differences between the excited states and the three-photon energy level. In Ar the lowest $ns'[1/2]_1$ ($4s'[1/2]_1$) state is much closer to the employed three-photon energies than any other state ($E(4s'[1/2]_1)=95\,400$ cm$^{-1}$, $E(4s[3/2]_1)=93\,751$ cm$^{-1}$, and $E(3d[1/2]_1)=111\,818$ cm$^{-1}$) [36]. The total cross section of the four-photon transitions to autoionizing states will consequently mainly consist of contributions of excitation routes in which this state is involved at the three-photon virtual level. In Xe, on the other hand, it is not only the lowest $ns'[1/2]_1$ ($6s'[1/2]_1$) state that is close to the three-photon energy ($E(6s'[1/2]_1)=77\,186$ cm$^{-1}$), but several other states ($E(6s[3/2]_1)=68\,046$ cm$^{-1}$, $E(5d[1/2]_1)=79\,987$ cm$^{-1}$, and $E(5d[7/2]_3)=80\,971$ cm$^{-1}$) [36] have comparable energy differences. For Xe more excitation routes are consequently expected to give significant contributions to the total four-photon excitation cross sections. Kr in this respect shows characteristics which are intermediate between Ar and Xe. The second aspect concerns the electronic character of the lowest $ns'[1/2]_1$ state in the three atoms. In Ar this state has almost exclusively $s'$ character [22], but it has been shown that in Xe the $6s'[1/2]_1$ state is heavily perturbed with $d$ and $d'$ character [26], while the lowest $ns'[1/2]_1$ state of Kr seems to show intermediate characteristics [2,25].

On the basis of the above the differences between the four-photon excitation spectra of Ar, Kr, and Xe can be explained consistently. First, these spectra show that the intensity of the resonances of the $np'$ series decreases as $n$ increases. This effect was most pronounced in Ar, which is in line with the observation that in Ar the three-photon energy is considerably closer to the lowest $ns'[1/2]_1$ state than any other excited state. In Kr and Xe excitation routes, which do not include the lowest $ns'[1/2]_1$ state, can therefore become significant. Second, our results show that in Xe the ratio $S_{J=2}/S_{J=4}$, determined for the $nf'$ resonances, exhibits a stronger excitation energy dependence than in Kr. This observation is in agreement with the electronic character of the lowest $ns'[1/2]_1$ state, which contains progressively more $d$ and $d'$ character in the series Ar, Kr, and Xe. Moreover, the behavior of the ratio $S_{J=2}/S_{J=4}$ is also influenced by the importance of excitation routes via states other than the lowest $ns'[1/2]_1$ state. In Xe more of such routes, for example, via the $5d[7/2]_3$ state, are possible and would consequently lead one to expect that in this atom $S_{J=2}/S_{J=4}$ is more susceptible to the excitation energy than in the other atoms. Finally, the four-photon excitation spectra of Ar have shown that for this atom the peak intensities of the $np'$ resonances are stronger than those of the $nf'$ resonances, while in Kr and Xe the reverse is found. This can again be understood qualitatively on the basis of the $d$ and $d'$ character involved at the three-photon virtual level, which affects the signal intensities of both the $np'$ and $nf'$ resonances. First, the cross section of the $nf'$ resonances increases as the three-photon virtual level contains more $d$ and $d'$ character. Second, the intensities of the $np'$ resonances are highly susceptible to the amount of $d$ and $d'$ character since the contributions to the total four-photon excitation cross section of the excitation routes which result from this particular electronic character may interfere destructively with the contributions of excitation routes which are due to $s'$ character. The possibility of such interferences has been suggested before [10].

## V. CONCLUSIONS

In the present study autoionizing states between the $^2P_{3/2}$ and $^2P_{1/2}$ ionic limits belonging to the $np'[1/2]_0$, $np'[3/2]_2$, $nf'[5/2]_2$, and $nf'[7/2]_4$ series of Ar, Kr, and Xe were studied in detail using four-photon excitation schemes. For Ar this study enabled the first observation of such autoionizing resonances, while for Kr and Xe previous experimental studies were improved on significantly by the use of both linearly and circularly polarized excitation light and by a better resolution.

All observed resonances were analyzed with the lineshape formula given in Eq. (1), enabling a quantitative description of the observed excitation spectra. The parameters $\mu_l$, $W_l$, and $q_l$ were compared, as far as possible, with those obtained in previous experimental and theoretical studies. Except for differences caused by the experimental conditions, the present results were found to be in reasonable agreement with previous experimental results. A comparison with theoretical calculations could, under the assumption of negligible closed-channel interactions, only be performed for the quantum defects and the width parameters. Except for the quantum defects of the $np'$ series in Xe, reasonable agreement was found.

The present study shows that the three-photon virtual level is of fundamental importance for a basic understanding of the observed relative intensities of the various resonances. On the one hand, the presence of real excited states close to this level causes near-resonance effects. On the other hand, it was found that the cross sections are to a major extent influenced by the electronic character of this level. It is clear that a detailed elucidation of all aspects considered in the present four-photon excitation work and in our previous three-photon excitation study, in which the odd $ns'[1/2]_1$, $nd'[3/2]_1$, $nd'[5/2]_3$, and $ng'[7/2]_3$ series have been accessed, would greatly benefit from high-quality theoretical MQDT calculations. It is hoped that the results of these two studies will provide further impetus for such calculations.

## ACKNOWLEDGMENTS

We gratefully acknowledge B. Rooswijk and Ing. D. Bebelaar for their technical skills, S. Woutersen for his theoretical assistance, and the Netherlands Organization for Scientific Research (NWO) for equipment grants and financial support.

[1] K. Radler and J. Berkowitz, J. Chem. Phys. **70**, 221 (1979).
[2] K. Yoshino and Y. Tanaka, J. Opt. Soc. Am. **69**, 159 (1979).
[3] K. Yoshino and D. E. Freeman, J. Opt. Soc. Am. B **2**, 1268 (1985).
[4] K. Ueda, K. Maeda, K. Ito, and T. Namioka, J. Phys. B **22**, L481 (1989).
[5] J. Z. Wu, S. B. Whitfield, C. D. Caldwell, M. O. Krause, P. van der Meulen, and A. Fahlman, Phys. Rev. A **42**, 1350 (1990).
[6] K. Maeda, K. Ueda, and T. Namioka, Phys. Scr. **41**, 464 (1990).
[7] K. Maeda, K. Ueda, T. Namioka, and K. Ito, Phys. Rev. A **45**, 527 (1992).
[8] K. Maeda, K. Ueda, and K. Ito, J. Phys. B **26**, 1541 (1993).
[9] J. P. Grandin and X. Husson, J. Phys. B **14**, 433 (1981).
[10] R. D. Knight and L. Wang, J. Opt. Soc. Am. B **2**, 1084 (1985).
[11] A. Wada, Y. Adachi, and C. Hirose, J. Phys. Chem. **90**, 6645 (1986).
[12] L. Wang and R. D. Knight, Phys. Rev. A **34**, 3902 (1986).
[13] A. Wada, Y. Adachi, and C. Hirose, J. Chem. Phys. **86**, 5904 (1987).
[14] D. Klar, K. Harth, J. Ganz, T. Kraft, M. W. Ruf, H. Hotop, V. Tsemekhman, K. Tsemekhman, and M. Ya. Amusia, Z. Phys. D **23**, 101 (1992).
[15] S. M. Koeckhoven, W. J. Buma, and C. A. de Lange, Phys. Rev. A **49**, 3322 (1994).
[16] P. R. Blazewicz, J. A. D. Stockdale, J. C. Miller, T. Efthimiopoulos, and C. Fotakis, Phys. Rev. A **35**, 1092 (1987).
[17] M. J. Proctor, J. A. D. Stockdale, T. Efthimiopoulos, and C. Fotakis, Chem. Phys. Lett. **137**, 223 (1987).
[18] W. E. Ernst, T. P. Softley, and R. N. Zare, Phys. Rev. A **37**, 4172 (1988).
[19] *CRC Handbook of Chemistry and Physics,* 66th ed., edited by R. C. Weast (CRC, Boca Raton, FL, 1986), p. E-259.
[20] C. J. Humphreys and E. Paul, J. Opt. Soc. Am. **60**, 1302 (1970).
[21] K. Ueda, Phys. Rev. A **35**, 2484 (1987).
[22] C. Lee and K. T. Lu, Phys. Rev. A **8**, 1241 (1973).
[23] J. Geiger, Z. Phys. A **282**, 129 (1977).
[24] W. R. Johnson, K. T. Cheng, K. N. Huang, and M. Le Dourneuf, Phys. Rev. A **22**, 989 (1980).
[25] K. T. Lu and U. Fano, Phys. Rev. A **2**, 81 (1970).
[26] K. T. Lu, Phys. Rev. A **4**, 579 (1971).
[27] M. Aymar, O. Robaux, and C. Thomas, J. Phys. B **14**, 4255 (1981).
[28] P. Gangopadhyay, X. Tang, P. Lambropoulos, and R. Shakeshaft, Phys. Rev. A **34**, 2998 (1986).
[29] A. L'Huillier, X. Tang, and P. Lambropoulos, Phys. Rev. A **39**, 1112 (1989).
[30] K. Ueda, J. Opt. Soc. Am. B **4**, 424 (1987).
[31] M. J. Seaton, Rep. Prog. Phys. **46**, 167 (1983).
[32] S. Geltman, J. Phys. B **13**, 115 (1980).
[33] Following S. E. Bialkowski and W. A. Guillory, Chem. Phys. **55**, 229 (1981), it can be shown that the ratio of the signal intensities obtained with circularly and linearly polarized excitation for a $J=4\leftarrow J=0$ four-photon transition is equal to $|A^4_{4,4}|^2/|A^4_{4,0}|^2$. In this expression $A^4_{4,q}$ is a component of the four-photon polarization tensor $\mathbf{A}^4$. Here $A^4_{4,4}=\langle 1111|22\rangle\langle 1122|33\rangle\langle 1133|44\rangle=1$ and $A^4_{4,0}=\langle 1010|20\rangle\langle 1020|30\rangle\langle 1030|40\rangle=(\frac{8}{35})^{1/2}$.
[34] M. Bounakhla, J. P. Lemoignet, J. P. Grandin, X. Husson, H. Kucal, and M. Aymar, J. Phys. B **26**, 245 (1993).
[35] O. L. Landen, M. D. Perry, and E. M. Campbell, Phys. Rev. Lett. **59**, 2558 (1987).
[36] C. E. Moore, *Atomic Energy Levels,* Natl. Bur. Stand. (U.S.) Circ. No. 35 (U.S. GPO, Washington, D.C., 1971), Vol. I, p. 211; *ibid.*, Vol. II, p. 169; *ibid.*, Vol. III, p. 113.